Urbach rule used to explain the variation of the absorption edge in $CdGeAs_2$ crystals

2005 J. Phys.: Condens. Matter 17 549

(http://iopscience.iop.org/0953-8984/17/3/013)

INSTITUTE OF PHYSICS PUBLISHING JOURNAL OF PHYSICS: CONDENSED MATTER

J. Phys.: Condens. Matter **17** (2005) 549–558 doi:10.1088/0953-8984/17/3/013

Urbach rule used to explain the variation of the absorption edge in $CdGeAs_2$ crystals

Lihua Bai[1], Chunchuan Xu[1], P G Schunemann[2], K Nagashio[3], R S Feigelson[3] and N C Giles[1,4]

[1] Physics Department, West Virginia University, Morgantown, WV 26506, USA
[2] BAE Systems, Nashua, NH 03061, USA
[3] Center for Materials Research, Stanford University, Stanford, CA 94305, USA

E-mail: Nancy.Giles@mail.wvu.edu

Received 2 October 2004, in final form 8 December 2004
Published 7 January 2005
Online at stacks.iop.org/JPhysCM/17/549

Abstract

The absorption edge has been studied over the temperature range from 5 to 300 K in both p-type and n-type bulk $CdGeAs_2$ crystals. An exponential distribution of states, or Urbach tail, below the direct band edge produces a linear dependence of $d[\log(\alpha)]/d(h\nu)$ with incident photon energy $h\nu$. The slope of this edge is nearly independent of temperature in p-type samples, but varies with temperature in n-type samples. These differences in behaviour are explained by a model that includes both thermal (phonon) and structural disorder contributions to the exponential tail of states. The structural disorder contribution was found to be dominant in compensated p-type samples. Indium-doped n-type $CdGeAs_2$ crystals exhibited the more conventional thermal (i.e., phonon) behaviour.

1. Introduction

Cadmium germanium arsenide ($CdGeAs_2$) is a direct-gap ternary chalcopyrite semiconductor with applications as a nonlinear optical material. It has a high nonlinear optical coefficient and thus is suitable for use in infrared frequency conversion devices. At room temperature, the transparency range of this material extends from about 2.3 μm to beyond 17 μm. Single crystals of $CdGeAs_2$, with sufficient size for fabricating optical devices, have been grown using the horizontal gradient freeze (HGF) technique [1–5]. As-grown bulk crystals of $CdGeAs_2$ are typically p-type, but the introduction of donor impurities can produce n-type material. The room-temperature direct band gap energy is about 0.57 eV [6]. The low-temperature band gap energy has been subject to some dispute over the years, with reported values ranging from 0.62 to 0.67 eV [7–10]. The presence of significant band tailing makes it difficult to determine the

[4] Author to whom any correspondence should be addressed.

band gap from absorption edge data. Additional complications arise because the absorption edge is polarized as a result of the chalcopyrite crystal structure [8]. Transitions from the highest valence band (V_1) to the conduction band are favoured for $\boldsymbol{E} \parallel c$, while transitions from the second highest valence band (V_2) to the conduction band are favoured for $\boldsymbol{E} \perp c$ [11].

An exponential absorption edge, or Urbach tail, is often observed in crystalline and amorphous materials [12–19]. Doping with impurities routinely alters the absorption edge, and it is often more appropriate to refer to an optical gap of a material, rather than the intrinsic electronic energy gap. Attempts have been made to present a general physical model to explain the origin of the commonly observed exponential absorption edge. Proposed models include effects due to microfields [20], exciton–phonon interactions [21, 22], and a combination of thermal (i.e., phonon) and structural disorders [23]. Structural disorder brings a temperature-independent term to the broadening of the absorption edge. The $CdGeAs_2$ crystals grown by the HGF technique contain large concentrations of both donor and acceptor defects [24], and thus potential fluctuations [25] are present in the conduction band and the valence band edges. These potential fluctuations provide a physical mechanism for structural disorder and are expected to play a role in explaining the Urbach tail in this material. We note that potential fluctuations have previously been shown to cause large energy shifts in the donor–acceptor-pair luminescence at 10 K in $CdGeAs_2$ [26].

In this study, the temperature dependence of the absorption edge was analysed for five $CdGeAs_2$ samples, two p-type and three n-type. We are able to fit our experimental results using the approach of Cody *et al* [23]. This gives an average phonon energy of 21 meV for $CdGeAs_2$. Structural disorder contributions to the exponential distribution of states are largest in the p-type compensated samples, while the tails of the absorption edge for n-type $CdGeAs_2$ samples are dominated by thermal contributions.

2. Experimental methods

The $CdGeAs_2$ samples used in this study were grown from nominally stoichiometric melts by the HGF technique at BAE Systems (Nashua, NH) and at Stanford University. Data were taken from five samples having varying conductivities. This sample set is representative of the large variation in optical absorption edge data observed for $CdGeAs_2$. Two of these samples are p-type and are typical of as-grown highly compensated crystals with large concentrations of native acceptors and donor impurities. The other three samples were cut from two boules intentionally doped with indium and are degenerately n-type. The indium impurity substitutes for the group II atom (i.e., Cd) in the II–IV–V_2 lattice and acts as a singly ionized donor. The samples were oriented and cut with faces perpendicular to the high-symmetry a and c directions. Four of the samples were c plates. Room-temperature Hall measurements were performed on these samples using the van der Pauw geometry with indium solder for electrical contacts. One of the p-type samples was an a plate, and van der Pauw Hall measurements could not be made due to the large anisotropy in conductivities along the a and c directions in this material. For this latter sample, the room-temperature hole concentration was estimated using the expression $p = (1.8{+}8.1\alpha) \times 10^{15}\ \mathrm{cm}^{-3}$ obtained from the data of a previous study [27] that reported the correlation between absorption at 0.22 eV (for $\boldsymbol{E} \perp c$) and Hall measurements. The sample thicknesses in our set varied from about 0.35 to 1.8 mm. Characteristics of these five samples (labelled A–E) are given in table 1.

Before the absorption measurements, the sample surfaces were mechanically polished using diamond paste down to 0.1 μm particle size. Data were then taken using a Fourier-transform infrared spectrometer (Thermo Nicolet Nexus 870) purged with nitrogen gas. A liquid-nitrogen-cooled HgCdTe detector and either a quartz or CaF_2 beamsplitter were used.

Table 1. Summary of information for the five $CdGeAs_2$ samples. Fitting parameters for the Urbach focus were obtained using equation (1), the parameters (S_0, $k\theta$, and X) describing the width of the absorption edge were obtained using equation (3), and the parameters S_g and $E_{opt}(0)$ were obtained using equation (4).

Sample	Thickness (mm)	Carrier concentration at 296 K (cm^{-3})	Urbach focus (E_0, α_0) (eV, cm^{-1})	S_0	$k\theta$ (meV)	X	S_g	$E_{opt}(0)$ (eV)
P-type								
A	0.35	5×10^{15}	$0.99, 1 \times 10^{16}$	0.10 ± 0.01	21 ± 2	10.3 ± 1.5	3.0 ± 0.1	0.63
B	1.40	2.7×10^{15}	$0.84, 1 \times 10^{11}$	0.14 ± 0.01	21 ± 3	6.7 ± 1.4	2.6 ± 0.2	0.63
N-type (doped with indium)								
C	1.04	-1.9×10^{18}	$0.87, 2.6 \times 10^{9}$	0.32 ± 0.02	21 ± 3	3.2 ± 0.7	4.7 ± 0.3	0.70
D	1.84	-2.7×10^{18}	$0.92, 2 \times 10^{10}$	0.29 ± 0.03	21 ± 6	3.1 ± 2.4	4.9 ± 0.6	0.71
E	1.84	-4.3×10^{18}	$0.82, 1.5 \times 10^{5}$	0.76 ± 0.03	21 ± 2	0.75 ± 0.2	3.7 ± 0.2	0.75

For the polarized absorption experiments on the a-plate sample, a wire-grid ZnSe polarizer was placed in the spectrometer before the sample to allow the $\boldsymbol{E}$ direction of the beam to be either parallel or perpendicular to the c axis. A continuous-flow helium cryostat (Oxford Instruments) was used to control the temperature of the samples in the range from 5 to 300 K. The measured absorbance (i.e., the optical density) was converted to absorption coefficient (α) values assuming that the reflectance R at a single surface for the spectral range investigated was constant. It has been reported that R varies only from about 0.34 to 0.36 [10, 28] near the band edge of $CdGeAs_2$, so this actual small variation in R corresponds to a maximum error of about 2 cm^{-1} in our determination of α values.

3. Results and discussion

Room-temperature absorption curves for two of our $CdGeAs_2$ samples are shown in figure 1. These data were taken with $\boldsymbol{E} \perp c$. The dashed curve is from an as-grown p-type sample (sample A). The solid curve is from an indium-doped n-type sample (sample E). The variation in absorption edge between the two samples illustrates the wide range in optical behaviour observed for $CdGeAs_2$ crystals having significantly different conductivities. The absorption edge for the heavily doped n-type sample is about 50 meV higher in energy. For the p-type sample, the long absorption tail extending beyond 0.2 eV contains contributions from other defect-related absorption bands. These transitions are weak compared to the absorption edge. The well-known discrete intervalence-band absorption (i.e., $V_2 \rightarrow V_1$) occurs near 0.22 eV (5.5 μm) in p-type $CdGeAs_2$ [29, 30]. Its intensity in this sample was about 0.4 cm^{-1} with $\boldsymbol{E} \perp c$. This intervalence-band absorption value corresponds to a hole concentration of about 5×10^{15} cm^{-3}. The n-type sample shown in figure 1 is degenerately doped and the Fermi level resides in the conduction band. The room-temperature electron concentration for this sample was 4.3×10^{18} cm^{-3}. The large concentration of free electrons in this n-type sample produces significant free-carrier absorption at energies less than 0.4 eV.

Optical transitions at the minimum direct-gap of $CdGeAs_2$ favour $\boldsymbol{E} \parallel c$, but we encounter an additional defect-related absorption near the band edge in p-type samples when this polarization is used. Thus, the data in figure 1 were taken with $\boldsymbol{E} \perp c$. To illustrate this point, we show a comparison of absorption curves taken from sample A with $\boldsymbol{E} \parallel c$ (solid curve) and with $\boldsymbol{E} \perp c$ (dashed curve) in figure 2. A discrete absorption band peaking near

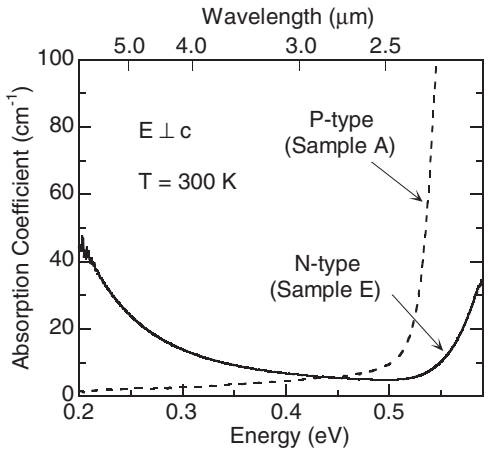

Figure 1. Room-temperature absorption coefficient data from p-type as-grown $CdGeAs_2$ (dashed curve) and n-type indium-doped $CdGeAs_2$ (solid curve). The data were taken with $\boldsymbol{E} \perp c$.

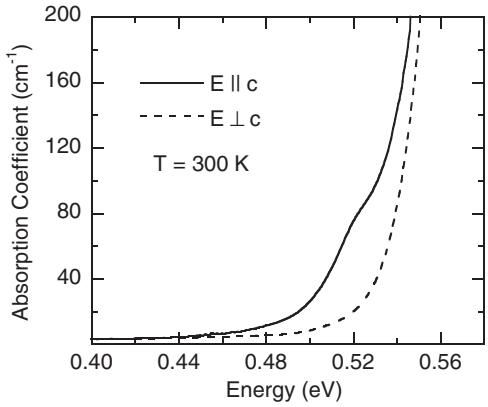

Figure 2. Polarization dependence of absorption for p-type $CdGeAs_2$ (sample A) at room temperature. The solid curve is taken with $\boldsymbol{E} \parallel c$ and the dashed curve is taken with $\boldsymbol{E} \perp c$.

0.53 eV is resolved in the $\boldsymbol{E} \parallel c$ spectrum. We attribute this discrete band to a transition from a shallow acceptor level to shallow donors and/or conduction band states. To avoid having this additional feature in our optical spectra, our analysis of the band edge absorption only uses spectra taken with $\boldsymbol{E} \perp c$. The transitions from the second highest valence band V_2 to the conduction band (i.e., transitions that are also favoured with $\boldsymbol{E} \perp c$) do not contribute in the spectral range where we obtain data, since their onset occurs at about 0.75 eV [11]. Thus, absorption-edge data taken with $\boldsymbol{E} \perp c$ from both p-type and n-type samples allow us to study the exponential tail of states below the lowest band gap of $CdGeAs_2$.

Figure 3 shows absorption data taken from sample A over the 5–300 K range using $\boldsymbol{E} \perp c$. These data are presented on a linear scale. The maximum value of approximately 200 cm^{-1} shown for α in figure 3 resulted from the absorbance limit of the spectrometer and the thickness of this sample. The absorption edge at 5 K occurs at about 0.6 eV, and then shifts to lower energies with increasing sample temperature. Ideally, the energy dependence for direct transitions should be proportional to $(h\nu - E_g)^{1/2}$, where E_g is the band gap energy and $h\nu$ is the incident photon energy. Instead, the experimental data indicate an exponential

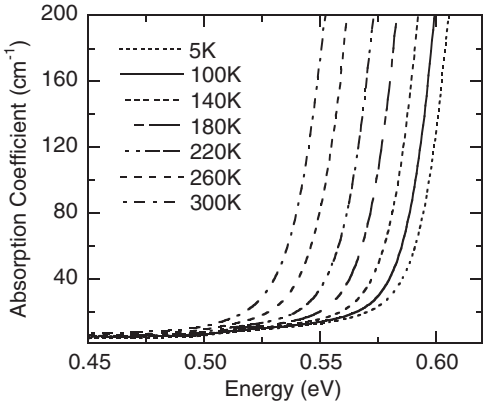

Figure 3. Temperature dependence of the absorption coefficient for p-type as-grown $CdGeAs_2$ (sample A). These data were taken with $\boldsymbol{E} \perp c$.

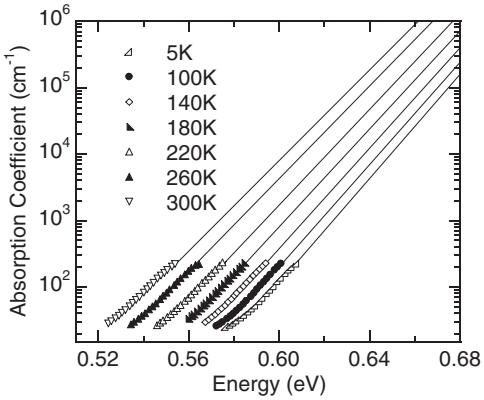

Figure 4. A semilog plot of the temperature dependence of the absorption coefficient for p-type $CdGeAs_2$ (sample A). The solid lines are the curve fits using equation (1). The converging point occurs at $(E_0, \alpha_0) = (0.99 \pm 0.04\ \text{eV}, 1 \times 10^{16}\ \text{cm}^{-1})$.

tail extending below E_g. This is better illustrated in figure 4. These same data form straight lines on a semilogarithmic plot, and are consistent with the Urbach rule [12].

The temperature dependence of the exponential relation between the absorption coefficient α and the incident photon energy $h\nu$ near the fundamental absorption edge is typically described by the following expression [13–15].

$$\alpha = \alpha_0 \exp\left[\frac{\sigma(h\nu - E_0)}{kT}\right]. \tag{1}$$

Here, α_0, E_0, and σ are fitting parameters with σ representing the steepness of the absorption edge. The extrapolations to higher energy of the absorption edge data taken at different temperatures converge to a point (or Urbach focus) described by the coordinates (E_0, α_0). We fit the sets of data represented by symbols in figure 4 to equation (1). The results are the solid lines shown in figure 4. The converging point for these lines was found to be approximately $(E_0, \alpha_0) = (0.99 \pm 0.04\ \text{eV}, 1 \times 10^{16}\ \text{cm}^{-1})$, which is off-scale for this plot. For this p-type material (sample A), the slope of the absorption edge changes very little as the temperature is increased from 5 to 300 K. A quite different result was obtained for n-type material (sample E).

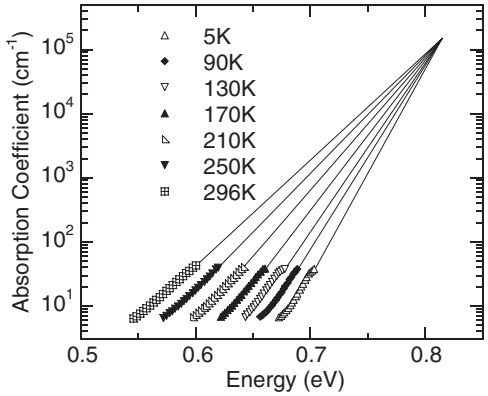

Figure 5. A semilog plot of the temperature dependence of the absorption coefficient for n-type $CdGeAs_2$ (sample E). The solid lines are the curve fits using equation (1). The converging point occurs at $(E_0, \alpha_0) = (0.815 \pm 0.025\ \text{eV}, 1.5 \times 10^5\ \text{cm}^{-1})$.

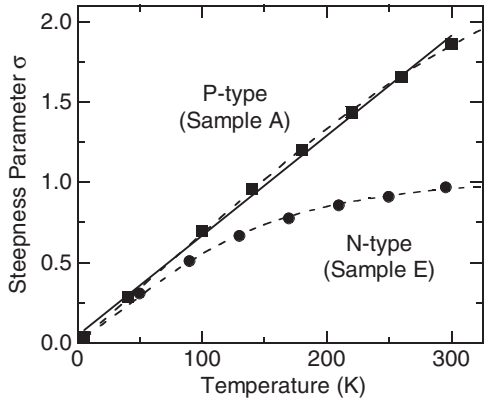

Figure 6. The steepness parameter σ as a function of temperature for p-type $CdGeAs_2$ (sample A) and n-type $CdGeAs_2$ (sample E). The dashed curves represent the best fits using equation (2). The solid line represents a linear fit for sample A.

Absorption data for sample E are shown in figure 5 on a semilogarithmic plot. In this case, the slope of the absorption edge decreased with increasing temperature. The curve fits for each temperature using equation (1) are shown as the solid lines in figure 5. The converging point was $(E_0, \alpha_0) = (0.815\ \text{eV} \pm 0.025\ \text{eV}, 1.5 \times 10^5\ \text{cm}^{-1})$. A similar analysis was done for the other three samples, and the results are given in table 1.

The temperature dependence of the steepness parameter σ is often used to determine the physical origins of contributions to the Urbach tail. We consider two separate approaches. In the first approach, we assume that the dominant cause for the Urbach tail is the exciton–phonon interaction. The steepness parameter σ then has the following temperature dependence [13, 31]:

$$\sigma = \sigma_0 \left(\frac{2kT}{\hbar\omega_\text{p}} \right) \tanh \left(\frac{\hbar\omega_\text{p}}{2kT} \right). \tag{2}$$

Here, $\hbar\omega_\text{p}$ corresponds to an average phonon energy, and the σ_0 parameter is sample dependent and inversely proportional to the strength of the phonon coupling [13]. In figure 6, the steepness parameters for the two representative samples A and E are shown as a function of temperature.

These values of σ were obtained when equation (1) was used to fit the data in figures 4 and 5. The dashed curves in figure 6 are the best fits to the discrete values of σ using equation (2). The fitting parameters obtained for p-type sample A are $\hbar\omega_p = 78$ meV (629 cm^{-1}) and $\sigma_0 = 3.08$. The fitting parameters for n-type sample E are $\hbar\omega_p = 32$ meV (258 cm^{-1}) and $\sigma_0 = 1.08$. As illustrated by the solid line in figure 6, a linear fit can also provide a reasonable description of the data from sample A.

The parameters $\hbar\omega_p$ are quite different for the two $CdGeAs_2$ samples described in figure 6, and this raises the question about the applicability of equation (2). The phonon modes for $CdGeAs_2$ observed in Raman spectroscopy and IR reflection experiments [32, 33] are in the range of 46–275 cm^{-1} (i.e., from 6 to 34 meV). The phonon energy value obtained for the n-type sample (sample E) is consistent with an optical phonon energy reported near 259 cm^{-1} [32] or 258 cm^{-1} [33]. However, for sample A, our extracted phonon energy is much greater than the reported values for $CdGeAs_2$. Also, we note that the constant σ_0 determined from the fitting process for sample A is about three times larger than the value determined for sample E. This latter parameter is inversely proportional to the strength of the phonon coupling, and this makes the exciton–phonon interaction in sample A, according to equation (2), three times smaller than in sample E.

It has been suggested that when the microfields, i.e., variations in the local electric fields, generated by phonons are small, the steepness parameter σ increases linearly with temperature and the slope σ/kT of the absorption edge is nearly constant with temperature [34]. If that is the case, the broadening of the absorption edge which gives rise to the exponential Urbach tail is mainly caused by structural disorder (e.g., from charged defects). The steepness parameter values for sample A closely follow a linear relation (indicated by the solid line in figure 6). This linear dependence of σ on temperature suggests that the thermal (phonon) disorder contribution to the Urbach tail is small in the compensated p-type sample. In contrast, the relation between σ and temperature is not linear for sample E, and this suggests that phonon coupling is more important in this sample compared to sample A.

Since the thermal (phonon) disorder model cannot account for the absence of temperature-dependent broadening of the absorption edge from the compensated p-type $CdGeAs_2$ sample A, we use a second approach [23] that includes two physically different contributions to the exponential absorption tail. One of these contributions is the previously described thermal disorder that reflects the temperature-dependent phonon participation. The other contribution is related to structural disorder, which is assumed to be independent of temperature, and is described by a dimensionless structural disorder parameter X. In this analysis, the width of the absorption edge is given by the parameter E_W which is related to the steepness parameter σ by the definition $E_W = kT/\sigma$. We use the σ values from figure 6 for the two $CdGeAs_2$ samples, and determine E_W at each measurement temperature. These results are shown as discrete data points in figure 7 for the two representative samples. From 5 to 300 K, the E_W values for the n-type sample varied from about 14 to 26 meV, while the variation for the p-type sample is only from about 12 to 14 meV.

The absorption edge energy width E_W is expressed as the sum of two contributions [17, 23]:

$$E_W(T) = S_0 k\theta \left(\frac{1+X}{2} + \frac{1}{\exp(\theta/T) - 1} \right). \tag{3}$$

Here, S_0 is a dimensionless coupling constant and $k\theta$ ($=\hbar\omega_p$) represents the average phonon energy in the material. The first term in equation (3) contains the disorder parameter X and is independent of temperature. The second term reflects the temperature-dependent phonon participation. This model has been previously employed to explain the absorption edge in semi-insulating and silicon-doped GaAs [17]. In the limit as $X \to 0$, equation (3) gives an E_W

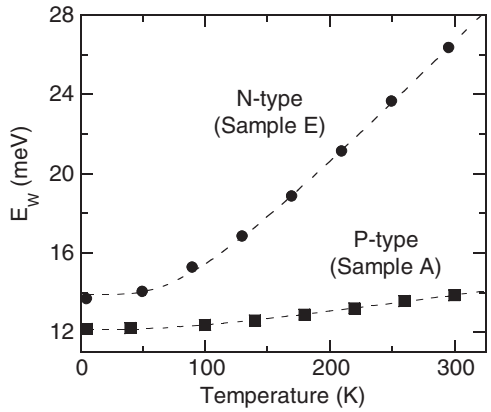

Figure 7. The absorption edge energy width E_W versus temperature for p-type $CdGeAs_2$ (sample A) and n-type $CdGeAs_2$ (sample E). The dashed curves represent the best fits using equation (3).

that when substituted into $\sigma = kT/E_W$ results in the expression for σ given by equation (2) if $\sigma_0 = (S_0)^{-1}$.

We use equation (3) to fit the discrete E_W values plotted in figure 7 for the two representative $CdGeAs_2$ samples. The dashed curves in figure 7 are the resulting curve fits. Similar procedures were followed for the other three samples, and the parameters S_0 and X and the average phonon energy $k\theta$ are given in table 1 for all five samples. The structural disorder parameter X is largest for the p-type samples A and B, and is much smaller for the highest-doped n-type sample E. If the structural disorder arises from potential fluctuations caused by a high density of charged defects, the reduced disorder in the n-type samples suggests that screening of the potential wells by free carriers has occurred. From the fitting, the average phonon energy $k\theta$ was found to be about 21 meV (169 cm^{-1}). By using an approach that includes both thermal and structural disorder contributions to the exponential absorption edge, we are able to account for the large variations observed in $CdGeAs_2$ absorption edge data. Even more importantly, we can use the same average phonon energy to describe the temperature behaviour of p-type and n-type samples.

The average phonon energy $k\theta$ found from an Urbach tail analysis is often used to describe the temperature variation of the material's optical band gap. In many cases, the electron–phonon contribution to the temperature variation of the band gap energy (E_g) can then be determined. For our set of five $CdGeAs_2$ samples, we proceeded as follows. At each measurement temperature, the absorption coefficient data were extrapolated to a value of about $\alpha \sim 1100$ cm^{-1}, corresponding to the absorption magnitude near the band gap [8, 10], and the energy position was noted. This value of absorption coefficient is the predicted absorption strength when photon energies exceeding the band gap by ~0.01 eV are used [35]. We then use these energy values as the optical band gap for a particular sample at a specific temperature T. The optical band gaps for the two samples A and E are plotted as a function of temperature in figure 8.

The optical band gap $E_{opt}(T)$ has the following relation with the average phonon energy [17, 36]:

$$E_{opt}(T) = E_{opt}(0) - S_g k\theta \left(\frac{1}{\exp(\theta/T) - 1} \right). \tag{4}$$

Here, S_g is a dimensionless 'coupling' constant and $E_{opt}(0)$ is the optical band gap at 0 K. The dashed curves in figure 8 represent the best fits using equation (4) and a phonon energy $k\theta$ of

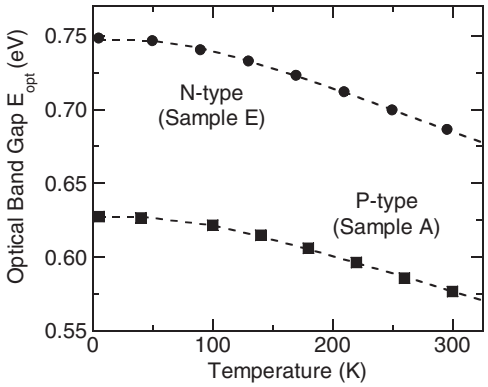

Figure 8. The optical band gap E_{opt} versus temperature for p-type $CdGeAs_2$ (sample A) and n-type $CdGeAs_2$ (sample E). The dashed curves represent the best fits using equation (4).

21 meV. The fitting parameters S_g and $E_{opt}(0)$ for the five samples are given in table 1. The coupling constant S_g varies from about 3 for the two p-type samples to as high as 5 for the n-type samples. The $E_{opt}(0)$ value is 0.63 eV in the two p-type samples. This is smaller than the $CdGeAs_2$ liquid-helium E_g value of 0.67 eV due to potential fluctuations [26]. The $E_{opt}(0)$ value increases from 0.70 to 0.75 eV with increasing electron concentration in the three n-type samples. These values are all larger than E_g because of conduction-band filling by the large concentrations of free electrons. Using the parameters S_g and S_0, the optical band gap can also be expressed in terms of the energy at the Urbach focus (E_0) and the absorption edge energy width (E_W).

$$E_{opt}(T) = E_0 - \frac{S_g}{S_0} E_W(T). \tag{5}$$

Then, the energy at the focal point E_0 will be larger than the $E_{opt}(0)$ value because it is shifted to higher energy by an amount equal to $\frac{S_g}{S_0} E_W(0)$. This shift is large in our p-type $CdGeAs_2$ samples.

4. Summary

Both p-type and n-type $CdGeAs_2$ samples were observed to have exponential absorption tails that follow the Urbach rule. The variation in absorption edge with temperature has been explained using a model including both structural disorder and thermal contributions. The structural disorder most likely comes from potential fluctuations caused by charged defects in the material. The effect of these potential fluctuations is stronger in compensated materials. Thus, in compensated p-type $CdGeAs_2$ (samples A and B), disorder is responsible for the slope that is nearly independent of temperature. In contrast, the disorder contribution is much smaller in the n-type indium-doped $CdGeAs_2$ (samples C through E) and the slope has a significant temperature dependence. The thermal contributions to the Urbach tail gave an average phonon energy of 21 meV in both p- and n-type material.

Acknowledgment

This work was supported by the Air Force Office of Scientific Research through MURI Grant No. F49620-01-1-0428.

References

[1] Schunemann P G and Pollak T M 1997 *J. Cryst. Growth* **174** 272
[2] Schunemann P G and Pollak T M 1997 Method for growing crystals *US Patent Specification* 5,611,856
[3] Schunemann P G and Pollak T M 1998 *Mater. Res. Soc. Bull.* **23** 23
[4] Schunemann P G, Setzler S D, Pollak T M, Ptak A J and Myers T H 2001 *J. Cryst. Growth* **225** 440
[5] Nagashio K, Watcharapasorn A, Zawilski K T, DeMattei R C, Feigelson R S, Bai L, Giles N C, Halliburton L E and Schunemann P G 2004 *J. Cryst. Growth* **269** 195
[6] Shileika A 1973 *Surf. Sci.* **37** 730
[7] Akimchenko I P, Ivanov V S and Borshchevskii A S 1973 *Sov. Phys.—Semicond.* **7** 309
[8] Rud Yu V and Tairov M A 1974 *Sov. Phys.—Semicond.* **8** 801
[9] Borshchevskii A S, Valov Yu A, Goryunova N A, Osmanov E O, Ryvkin S M and Shpen'kov G P 1969 *Sov. Phys.—Semicond.* **2** 1145
[10] Akimchenko I P, Borshchevskii A S and Ivanov V S 1973 *Sov. Phys.—Semicond.* **7** 98
[11] Shay J L and Wernick J H 1975 *Tenary Chalcopyrite Semiconductors: Growth, Electronic Properties, and Applications* (New York: Pergamon)
[12] Urbach F 1953 *Phys. Rev.* **92** 1324
[13] Chichibu S, Mizutani T, Shioda T and Nakanishi H 1997 *Appl. Phys. Lett.* **70** 3440
[14] Abay B, Guder H S, Efeoglu H and Yogurtcu Y K 1998 *J. Appl. Phys.* **84** 3872
[15] Medvedkin G A, Rud Yu V and Tairov M A 1989 *Phys. Status Solidi* a **111** 289
[16] Redfield D and Afromowitz M A 1967 *Appl. Phys. Lett.* **11** 138
[17] Johnson S R and Tiedje T 1995 *J. Appl. Phys.* **78** 5609
[18] Rincon C, Wasim S M, Marin G, Marquez R, Nieves L, Sanchez Perez G and Medina E 2001 *J. Appl. Phys.* **90** 4423
[19] He T, Ehrhart P and Meuffels P 1996 *J. Appl. Phys.* **79** 3219
[20] Dow J D and Redfield D 1972 *Phys. Rev.* B **5** 594
[21] Sumi H and Toyozawa Y 1971 *J. Phys. Soc. Japan* **31** 342
[22] Schreiber M and Toyozawa Y 1982 *J. Phys. Soc. Japan* **51** 1544
[23] Cody G D, Tiedje T, Abeles B, Brooks B and Goldstein Y 1981 *Phys. Rev. Lett.* **47** 1480
[24] Ptak A J, Jain S, Stevens K T, Myers T H, Schunemann P G, Setzler S D and Pollak T M 2000 *Mater. Res. Soc. Symp. Proc.* **607** 427
[25] Pankove J I 1971 *Optical Processes in Semiconductors* (New York: Dover)
[26] Bai L, Giles N C, Schunemann P G, Pollak T M, Nagashio K and Feigelson R S 2004 *J. Appl. Phys.* **95** 4840
[27] Bai L, Garces N Y, Yang N, Schunemann P G, Setzler S D, Pollak T M, Halliburton L E and Giles N C 2003 *Mater. Res. Soc. Proc.* **744** 537
[28] Hong K S, Speyer R F and Condrate R A Sr 1990 *J. Phys. Chem. Solids* **51** 969
[29] Mamedov B Kh and Osmanov E O 1972 *Sov. Phys.—Semicond.* **5** 1120
[30] Bai L, Poston J A Jr, Schunemann P G, Nagashio K, Feigelson R S and Giles N C 2004 *J. Phys.: Condens. Matter* **16** 1279
[31] Kurik M V 1971 *Phys. Status Solidi* a **8** 9
[32] Pascual J, Pujol J, Artus L and Camassel J 1991 *Phys. Rev.* B **43** 9831
[33] Abtropova E V, Kopytov A V and Poplavnoi A S 1988 *Opt. Spectrosc. (USSR)* **64** 766
[34] Brada Y and Roth M 1989 *Phys. Rev.* B **39** 10402
[35] Bai L 2004 Optical properties of $CdGeAs_2$ *PhD Dissertation* West Virginia University, chapter 2
[36] Cody G D 1984 *Semiconductors and Semimetals* part B, vol 21, ed J I Pankove (New York: Academic) chapter 2